

Biophysical Journal, Volume 98

Supporting Material

Theoretical analysis of the F1-ATPase experimental data

Ruben Perez-Carrasco and Jose Maria Sancho

MS ID: BIOPHYSJ/2009/172502

MS TITLE: Theoretical analysis of the F1-ATPase experimental data

Supporting Material

S1. Dependence of the model with ATP hydrolysis energy

The flashing ratchet model presented here is able to lead successfully in the case of taking ΔG_{ATP} as an experimental variable. Recent experiments use ΔG_{ATP} as a control parameter (8). Since the potential relaxed state must be independent of the ATP hydrolysis, the rest state parameter V_0 has to be fixed, but the parameter V_1 of excited potential has to depend on ΔG_{ATP} . Here, we extend the previous calculation to consider this important change,

The energy conservation constraint (Eqs. 8) reads now ,

$$\Delta G_{ATP} = E_1 + E_2 = \frac{2\alpha}{1+2\alpha}V_1 + 2(1-\alpha)V_0 \quad (\text{S.1})$$

$$= \left(\frac{2\alpha\varepsilon}{1+2\alpha} + 2(1-\alpha) \right) V_0, \quad (\text{S.2})$$

where the adimensional energy parameter $\varepsilon \equiv \frac{V_1}{V_0}$ has been used.

For this system the total mechanical time reads,

$$t_{mech} = \left(\frac{2\pi}{3} \right)^2 \frac{(\gamma + \gamma_L)}{\Delta G_{ATP}} \left(\frac{\alpha\varepsilon}{1+2\alpha} + 1 - \alpha \right) \left(\frac{\alpha(1+2\alpha)}{\varepsilon} + 1 - \alpha \right) \quad (\text{S.3})$$

which achieves a maximum value for different values of ε ,

$$\varepsilon = -5 + 6\alpha_M + \frac{-6 + 12\alpha_M}{-1 + 2\alpha_M(1 + \alpha_M)}. \quad (\text{S.4})$$

On the other hand, from the energy conservation relation (Eq. S.2) one gets another relation between the different parameters,

$$\varepsilon(\alpha, \Delta G/V_0) = \left(1 + \frac{1}{2\alpha} \right) \left(\frac{\Delta G}{V_0} - 2(1 - \alpha) \right) \quad (\text{S.5})$$

From the conditions S.4 and S.5 it can be obtained the optimum value of α_M that corresponds to a certain ratio $\Delta G_{ATP}/V_0$ (Fig. S.1). Thus, once V_0 is fixed it can be obtained a relation $\alpha_M(\Delta G_{ATP})$ and the different torques and times related with it.

This analysis predicts that the substep sizes do depend on the energy hydrolysis in a range not too far from the experimental observations. Furthermore, this more complete description changes the original energetic parameters of the motor, being more appropriate a height for the relaxed potential of $V_0 = 70$ pN nm. This prediction and the associated torques could be tested if the experimental resolution of the substeps angles is improved.

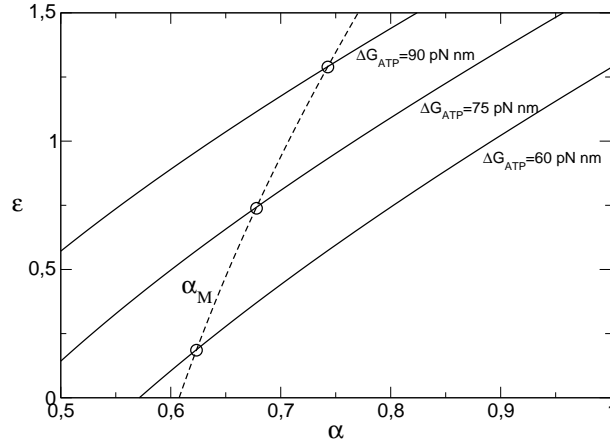


Figure S.1. The corresponding value of α_M can be found as the intersection between the α_M relation (Eq. S.4) (*dashed line*) and the energy conservation relation (Eq. S.5) (*solid lines*). $V_0 = 70$ pN nm.

S2. Coupling ratio estimation

The coupling ratio measures the average number of successful steps produced by an ATP hydrolysis. Starting with the shaft in one minimum of the relaxed potential it begins to advance when the potential is switched to the excited state. Once the time t_E is over, the fraction of the tail of the angular distribution probability of the shaft that doesn't reach the next relaxing dip will relax back to the same initial minimum rest state. This fraction of the probability distribution indicates the probability of obtaining a failed step (Fig. 9). Thus the problem of studying analytically the coupling ratio is reduced to study the evolution of an initial distribution corresponding to the dip of the rest state over the excited potential during a time t_E . Since all the parameters of the systems are determined, the probability density is the solution to the following Fokker-Planck equation,

$$\partial_t P_E(\theta, t) = \frac{1}{\gamma + \gamma_L} \partial_\theta [V'_E(\theta) + k_B T \partial_\theta] P_E(\theta, t) \quad (\text{S.6})$$

Nevertheless the problem is still complex since the solution for such a non-linear potential is not straightforward. Since the interest in the problem is at the left tail of the distribution (Fig. 9), the potential can be replaced by a linear potential i.e. a constant torque τ_1 is applied over the whole trajectory. This approximation ignores a priori the effects of the reflecting part of the excited potential (this approximation will be reviewed later). In addition, the angular distribution of the shaft will be approximated by a gaussian distribution function in order to simplify the calculations.

The initial angular probability distribution function in the relaxed state can be obtained solving the Fokker-Planck equation in one of the minimums (centered at $x = 0$)

of the relaxed potential,

$$\left. \begin{aligned} 0 &= -\tau_2 d_\theta P_R(\theta) + k_B T d_\theta^2 P_R(\theta) \quad , \theta < 0 \\ 0 &= \tau_2 d_\theta P_R(\theta) + k_B T d_\theta^2 P_R(\theta) \quad , \theta > 0 \end{aligned} \right\} \quad (\text{S.7})$$

The solution for these second order linear homogeneous equations are two exponentials. Imposing as a boundary conditions the continuity of the probability at $\theta = 0$ and its normalization, the final expression is,

$$P_R(\theta) = \begin{cases} \frac{1}{2} \frac{\tau_2}{k_B T} e^{\frac{\tau_2}{k_B T} \theta} & , \theta < 0 \\ \frac{1}{2} \frac{\tau_2}{k_B T} e^{-\frac{\tau_2}{k_B T} \theta} & , \theta > 0 \end{cases} \quad (\text{S.8})$$

From it can be extracted the different statistics needed (average and variance) in order to describe the approximated initial gaussian distribution,

$$\langle \theta \rangle_0 = 0 \quad (\text{S.9})$$

$$\begin{aligned} \langle (\theta - \langle \theta \rangle)^2 \rangle_0 &= \langle \theta^2 \rangle_0 = \frac{\tau_2}{k_B T} \int_0^\infty \theta^2 e^{-\frac{\tau_2}{k_B T} \theta} d\theta \\ &= 2 \left(\frac{k_B T}{\tau_2} \right)^2 \end{aligned} \quad (\text{S.10})$$

So the initial probability just before the flashing of the potential can be approximated by,

$$P_E(\theta, 0) = \frac{1}{\sqrt{4\pi}} \frac{\tau_2}{k_B T} e^{\left(\frac{\tau_2}{2k_B T} \theta\right)^2} \quad (\text{S.11})$$

Since it is proposed a constant torque for the gaussian profile to advance, the time evolution will still be gaussian and therefore we only need the evolution of the mean value and the variance of the probability distribution function in order to find an expression for $P_E(x, t)$. This can be obtained directly from the formal solution for the trajectory extracted from the Langevin equation of the shaft (Eq. 20)

$$\theta = \theta_0 + \frac{1}{\gamma_{eff}} \int^t (\tau_1 + \xi) dt \quad (\text{S.12})$$

Obtaining the mean value,

$$\langle \theta \rangle = \frac{\tau_1 t}{\gamma_{eff}}, \quad (\text{S.13})$$

and the variance,

$$\langle \Delta \theta^2 \rangle = 2 \left(\frac{k_B T}{\tau_2} \right)^2 + \frac{2k_B T}{\gamma_{eff}} t \quad (\text{S.14})$$

Finally, the computation of the coupling ratio is the fraction of the gaussian that is placed at the right of the next maximum of the excited potential $\theta_c = \pi/3$ at a time t_E (figure 9).

$$\begin{aligned} cr(\gamma_L) &= \int_{\theta_c}^\infty P_E(\theta, t_E) d\theta = \\ &= \frac{1 + \text{fer}(\mu_c)}{2}, \end{aligned} \quad (\text{S.15})$$

with,

$$\mu_c = \frac{\langle \theta \rangle - \theta_c}{\sqrt{\langle \Delta \theta^2 \rangle}} \Big|_{t_E}. \quad (\text{S.16})$$

This expression for the coupling ratio results in a good approximation for values of the load above 0.01 pNnm. It is worth to study carefully the dependence of the coupling ratio with the friction of the load along the excitation time t_E . Since the mechanical time t_{mech1} is proportional to the effective friction coefficient $(\gamma + \gamma_L)$ (Eq. 14), the evolution of the probability density function does not depend on the friction of the load during this first evolution period. The difference comes in the waiting step of duration t_0 . Since t_0 is independent of the friction of the load and the dynamics of the system with a lower friction are quicker to that of a system with a bigger load, the shrink of the left tail of the probability distribution function will be greater the smaller is the friction, increasing thus the coupling ratio of the motor.

Nevertheless, no matter the smaller the friction of the load is, the motor has a saturating coupling ratio different from one (Fig. 10). This is so due to the fact that the effects of the reflecting force of the minimum neglected in the former calculation are significant. Altogether one can compute the limit coupling ratio imposed by this reflecting force from the stationary distribution for the minimum of the excited potential, in such a way that the intrinsic coupling ratio of this distribution will be an upper limit for $cr(\gamma_L)$, i.e., the left queue will not advance more than its stationary value. Since it is a stationary distribution this limit value will not depend on the friction of the system but on its geometry. Solving the FP equation for this minimum in the same way as the previous one, it is found the stationary solution:

$$P_E^\infty(\theta) = \begin{cases} \frac{\tau_3 \tau_2}{\tau_2 + \tau_3} e^{\frac{\tau_2}{k_B T} \theta} \\ \frac{\tau_3 \tau_2}{\tau_2 + \tau_3} e^{-\frac{\tau_3}{k_B T} \theta} \end{cases} \quad (\text{S.17})$$

Being τ_3 the torque of the reflecting torque. The corresponding coupling ratio for this probability profile is,

$$cr^0 = \int_{\theta_c}^{\infty} P_E^\infty(\theta) d\theta = \frac{\tau_3 \tau_2}{\tau_2 + \tau_3} e^{\frac{\tau_2}{k_B T} \theta_c}, \quad (\text{S.18})$$

That for the values of the parameter using in the simulation returns an upper limit for the coupling ratio of $cr^0 \simeq 0.96$ in agreement with the simulations of the system.

This result can be used in order to obtain a final approximation for the coupling ratio it can be written in a compact analytical way by interpolating Eq. S.15 with the maximum value cr^0 (Eq. S.18),

$$CR(\gamma_L) = \frac{cr(\infty)(1 - cr^0)}{1 - cr(\infty)} + \frac{cr^0 - cr(\infty)}{1 - cr(\infty)} cr(\gamma_L), \quad (\text{S.19})$$

which gives a good prediction for the coupling ratio of the motor.

S3. Dependence of the velocity of the motor with the stiffness κ

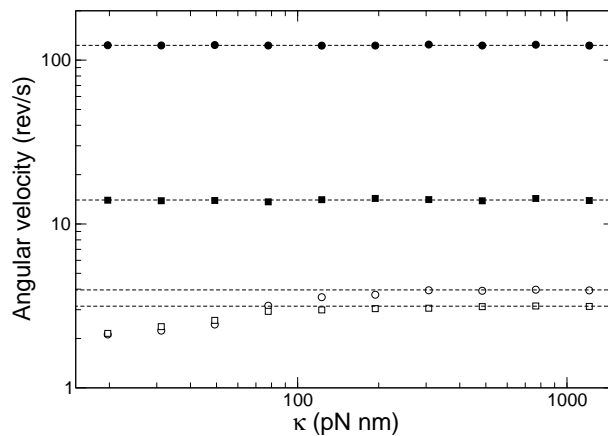


Figure S.2. Dependence of the mean angular velocity with the stiffness of the joint shaft-load κ . The dependence has been studied for different values of the load friction, $\gamma_L = 1$ pN nm s (*squares*) and $\gamma_L = 0.0002$ pN nm s (*circles*), and for different values of [ATP], [ATP]=2 μ M (*open*) and [ATP]=2 mM (*solid*). The dashed line corresponds with simulations of the rigid coupling limit (Eq. 20). For values of the stiffness of 200 pN nm or greater the results fits well with the rigid coupling.